Scientific paper

Structures and Properties of Phenylethanoid Glycosides from *Barleria prionitis* Linn.: Insights from Theoretical and Experimental Investigations

Onesy Keomanykham,^{1,2} Hue Van Nguyen,^{1,3} Le Thi Phuong Hoa,⁴ Nguyen Xuan Ha,⁵ Bounnam Xangyaorn,² Hue Minh Thi Nguyen^{1,3} and Dang Ngoc Quang^{1,*}

¹ Faculty of Chemistry, Hanoi National University of Education, 136-Xuan Thuy, Hanoi, Vietnam

² Luangnamtha Teacher Training College, Luang Namtha, Laos

³ Center for Computational Science, Hanoi National University of Education, 136-Xuan Thuy, Hanoi, Vietnam

⁴ Faculty of Biology, Hanoi National University of Education, 136-Xuan Thuy, Hanoi, Vietnam

⁵ Institute of Natural Products Chemistry, Vietnam Academy of Science and Technology, 18 Hoang Quoc Viet, Cau Giay, Hanoi, Vietnam

* Corresponding author: E-mail: quangdn@hnue.edu.vn

Received: 10-15-2024

Abstract

Six phenylethanoid glycosides, acetylmartynoside A (1), martynoside (2), 3-O-methylpoliumoside (3), isoaceteoside (4), leucosceptoside A (5), 2-(3-hydroxy-4-methoxyphenyl)-ethyl-O-(α -L-rhamnosyl)-(1 \rightarrow 3)-O-(α -L-rhamnos-yl)-(1 \rightarrow 6)-4-O-E-feruloyl- β -D-glucopyranoside (6) were isolated for the first time from the whole plant of Barleria prionitis Linn. Their structures were elucidated by 1D and 2D NMR and mass spectra. In addition, the antioxidant activity of compounds 1-6 was investigated. All of the compounds showed Keap1 protein inhibitory effects with estimated binding affinities in the range of -9.639 to -9.084 kcal/mol by molecular docking and moderate DPPH free radical scavenging activity with their IC₅₀ values in the range of 110–389 μ M. Furthermore, the predicted toxicity results of all six compounds 1-6 indicated a level of 5 and a high LD₅₀ value (LD₅₀ = 5000 mg/kg), which showed low toxicity and high safety for oral consumption in humans.

Keywords: Barleria prionitis, antioxidant activity, density functional theory, molecular docking, toxicity prediction

1. Introduction

Baleria prionitis Linn. (Acanthaceae) is a perennial shrub, 1–2 meters high, widely distributed throughout Africa, India, Sri Lanka and tropical Asia such as China, Myanmar, Vietnam, Thailand, and Laos. 1–4 *B. prionitis* has been used extensively in folk medicines in several countries, such as Vietnam and Laos, for the treatment of many common diseases such as cough, cold, sore throat, hyperhidrosis, detoxification, tooth decay, hemorrhoids, dermatitis, inflammation of the lymph nodes, viral infection, snake bite, stomach disorders, urinary infection, catarrh, fever in children and cancer. 5–7 Phytochemical investigations of this plant revealed iridoid glycoside, phenylethanoid glycoside, flavonoid, terpenoid, and phenolic acid

as its main chemical constituents. 8-11 The crude extracts of this plant have been reported for their biological activity against respiratory syncytial virus, anti-inflammatory, antimicrobial, antidiabetic, anticancer, hepatoprotective, immunorestorative, and especially antioxidant properties. 12-18 Recently, barlerinoside, phenylethanoid glycoside from this plant, showed strong radical scavenging activity in a DPPH assay with an IC₅₀ value of 0.41 mg/mL. 8 These findings encourage us to investigate its antioxidant constituents, especially the sample collected in Laos that hasn't been studied yet for its chemical constituents and biological activities. Theoretical calculations based on the Density Functional Theory (DFT) method have emerged as a powerful technique for assessing structural properties and understanding the electronic interaction be-

tween a studied molecule and its target receptor. Numerous DFT studies have been published describing a range of properties of phenylethanoids. 19-20 The molecular docking approach is an effective strategy-to gain a deeper understanding of ligand-receptor interactions and screen natural compounds. The significant role of molecular docking in drug discovery lies in its ability to predict the optimal binding mode between natural compounds and target proteins. Molecular docking methods have been widely employed to analyze the biological activities of phenylethanoids.^{21–24} Recent theoretical studies using DFT and molecular docking have highlighted the significance of analyzing ligand-receptor interactions, especially between natural compounds and target proteins like Keap1.^{25,26} Keap1, a key regulator of the Nrf2 pathway, plays a crucial role in cellular antioxidant defense mechanisms. By targeting Keap1, natural phenylethanoids from B. prionitis could potentially enhance Nrf2 activation, offering a promising strategy for combating oxidative stress-related diseases.²⁷ Therefore, Keap1 was chosen as the target receptor for the molecular docking studies in this research. This paper describes the isolation, structural elucidation, theoretical, and experimental studies on the antioxidant activity of six phenylethanoid glycosides from Barleria prionitis collected in Luangnamtha, Laos.

2. Experimental

2. 1. General

Thin layer chromatography (TLC) was carried out on pre-coated Si gel GF254 (Merck). TLC spots were viewed at 254, 302 and 365 nm and visualized by spraying with 10% H₂SO₄ in methanol followed by heating until the spots appeared. Column chromatography was carried out on silica gel 60 Ao(60-100 μm, Merck), Sephadex LH-20 (Amersham Pharmacia Biotech) and Diaion HP-20 (Supelco). Preparative medium-pressure liquid chromatography (MPLC) was performed with a Work-21 pump (Lab-Quatec Co., Ltd, Japan) and a reversed phase (C-18) Lobar column (Merck), a flow rate of 1.0 mL/min. Preparative-High performance liquid chromatography (Prep. HPLC) was performed on a Jasco PU-2087 instrument with a UV-2070 and RI-2031 detectors using a Waters 5C 18-AR-II column (10.0 \times 250 mm), flow rate of 1.0 mL/ min. 1D and 2D NMR (1H, 13C NMR, HSQC, HMBC and ROESY) spectra were recorded on a Bruker Avance 600 MHz Instrument. The mass spectra were obtained on a UPLC-ESI S4SH8000 (Water).

2. 2. Plant Material

The whole plant of *Baleria prionitis* was collected in Luang Namtha province, Laos from July to December in 2021 and identified by Bounnam XANGYAORN, Luangnamtha Teacher Training College, Luangnamtha, Laos.

Voucher specimen (BP2021) has been deposited at Faculty of Chemistry, Hanoi University of Education, Vietnam.

2. 3. Extraction and Isolation

The whole dried plant of B. prionitis (10.0 kg) was powdered and extracted five times with methanol (each 20 L) to afford the crude methanol extract (922 g), which was partitioned between *n*-hexane, EtOAc, butanol and water. The EtOAc extract (64 g) was subjected to silica gel column, using n-hexane/EtOAc gradient (from 2/1 to 1/1, v/v) and EtOAc/MeOH (from 98:2 to 80:20 v/v) to give 10 fractions (BPE1-10). Fraction BPE5 (4.1335 g) was further isolated by silica gel column, using a gradient elution of CHCl₃/MeOH (from 40:1 to 7:1, v/v) to give 12 sub-fractions (BPE5A-L). Sub-fraction BPE5I (93.4 mg) was separated by MPLC, using a solvent system of CH₃CN/H₂O (2:3, v/v) to yield compound 1 (22 mg). Fraction BPE7 (4.5 g) was subjected to Sephadex LH-20 column, eluting with MeOH/CHCl₃ (7:3, v/v) to give 7 sub-fractions (BPE7A-G). Sub-fraction BPE7B (3.2 g) was further chromatographed on a silica gel column, eluting with CHCl₃/MeOH/H₂O gradient (from 25:2:0.1 to 25:3.5:0.1, v/v/v) to give 13 sub-fractions (BPE7B1-13). Then sub-fraction BPE7B12 (181 mg) was purified by MPLC, MeOH/H₂O (6:4, v/v) to yield compound 2 (27.8 mg).

The BuOH extract (147 g) was subjected to Diaion HP-20 column, eluting with H₂O 100%, H₂O/MeOH gradient (from 95:5 to 30:70, v/v) and MeOH 100% to give 12 fractions (BPB1-12). Fraction BPB9 (298 mg) was further isolated by MPLC, using a solvent system of CH₃CN/H₂O (25:75, v/v) to give 4 sub-fractions (BPB9A-D). Sub-fraction BPB9A (53.5 mg) was further chromatographed on Sephadex LH-20 column, eluting with MeOH 100%, followed by a silica gel column, CHCl₃/MeOH/H₂O (25:7:0.1, v/v/v) to yield compound 3 (4.8 mg). Sub-fraction BPB9B (36 mg) was isolated by HPLC with a reversed phase column (C-18), using solvent system of CH₃CN/H₂O (25:75, v/v), rt. 60.12 min. to give sub-fraction BPB9B2, which was further isolated by Sephadex LH-20 column, MeOH 100% to afford 4 (2.7 mg). Sub-fraction BPB9C (45.6 mg) was purified by Sephadex LH-20 column, eluting with MeOH 100%, followed by HPLC, EtOAc/MeOH/H2O (10:1:0.1, v/v/v), rt. 25.30 min. to yield compound 5 (3 mg). Finally, compound 6 (12.4 mg) was obtained from sub-fraction BPB9D (63 mg) by Sephadex LH-20 column, MeOH 100%, followed by a silica gel column, with solvent system of CHCl₂/MeOH/H₂O (25:5:0.1, v/v/v).

2.4. Density functional theory, molecular docking and oral toxicity prediction studies

The 2D and 3D chemical structures of isolated compounds (1-6) from *B. prionitis* were generated using ChemSketch software. Subsequently, the geometry of phe-

nylethanoid glycosides was optimized based on density functional theory (DFT) with the B3LYP/6-311g(d, p) theoretical level using Gaussian 09 software. The HOMO-LUMO diagram was visualized using VMD software, and the molecular electrostatic potential (MEP) map of the molecule was computed and displayed using Gauss-View 06 software. The energy gap ΔE was calculated as the difference between the LUMO and HOMO energies, indicating the potential electron transfer from the ground state to the excited state of the molecule.

For protein target preparation, the crystal structure of Kelch-like ECH-associated protein 1 (Keap1) (PDB entry: 4L7B) was downloaded in *.pdb format from the RCSB Protein Data Bank (https://www.rcsb.org/structure/4L7B). ²⁹ In the downloaded file, PyMOL v.2.5.7 software was used to visualize and remove water molecules, ions, and co-crystallized molecules. The Keap1 protein structure was supplemented with hydrogen atoms and subjected to Kollman calculations. All ligand and protein files were saved in *pdbqt format for the docking process. Docking parameters were set, including the grid box center and size based on the centroid of the co-crystallized

ligand and coverage of important amino acids. An exhaustiveness value of 400 was chosen, and docking simulation was performed using AutoDock Vina v1.2.3.³⁰ The results of the interaction analysis between compounds (**1-6**) and Keap1 residues were visualized using Discovery Studio Visualizer software.

The toxicity prediction of the studied compounds was also conducted to assess their toxicity levels and predict the lethal dose (LD_{50}) using the ProTox 3.0 web server.³¹

2. 5. Biological Assays

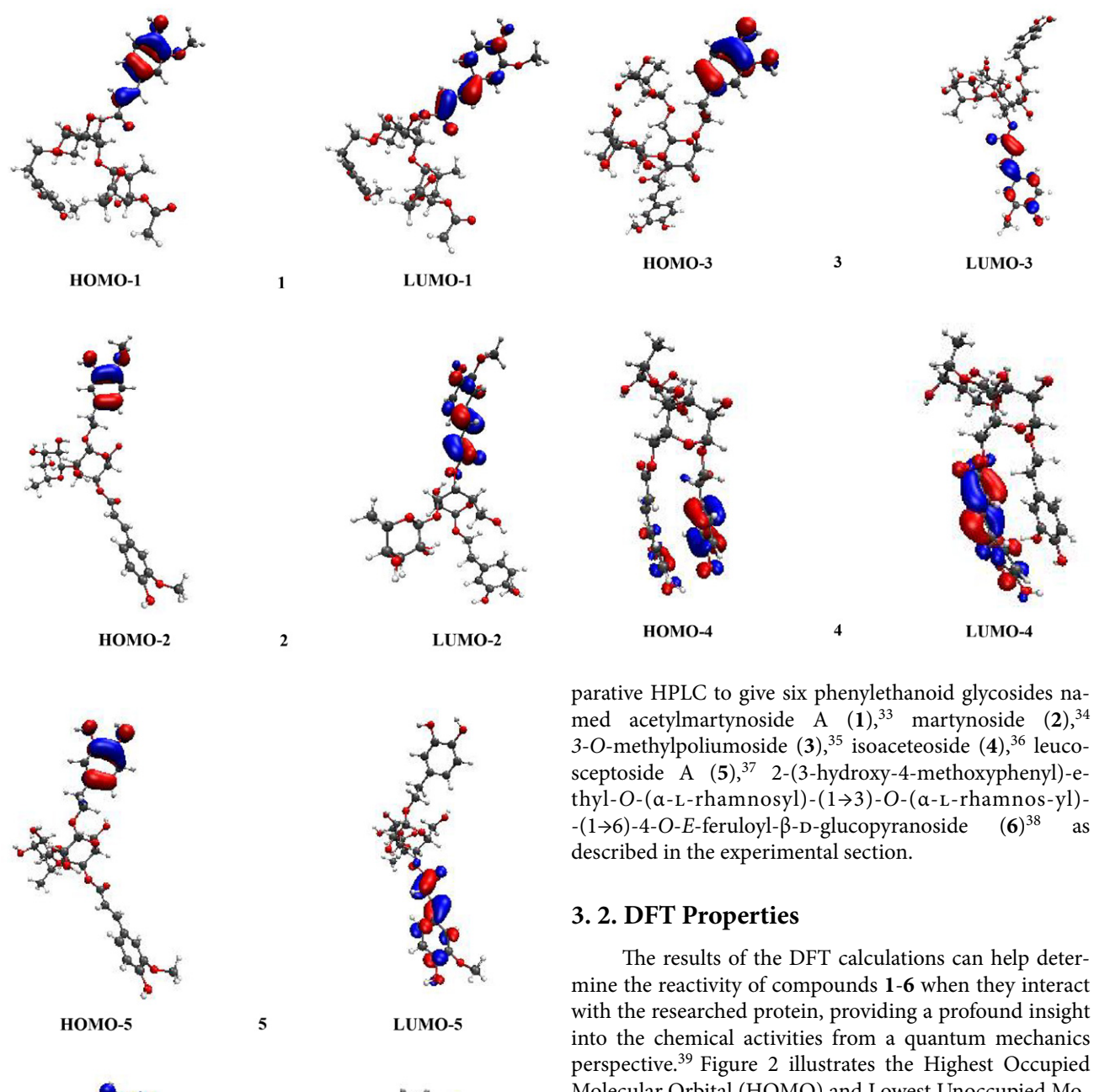
Free radical scavenging activity was determined using DPPH as a reagent.³²

3. Results and Discussion

3. 1. Chemistry

The methanolic extract of *B. prionitis* L. was divided into four fractions, and followed by silica gel, sephadex LH-20, Diaion HP-20 column chromatography, and pre-

Figure 1. Chemical structures of compounds 1-6 from B. prionitis



ment, the concepts of HOMO and LUMO are crucial for understanding the electronic properties of molecules. HO-MO represents the tendency for electrons, while LUMO represents the opposite.³⁹ As observed in Figure 2, the HOMO representation of 2, 3, 4, 5, and 6 is mainly distributed over the benzene ring and the oxygen atoms attached to this ring of the phenethyl alcohol group, while 1 concentrates its distribution on the trans-feruloyl group, with номо-6 LUMO-6 4 distributing over both benzene rings in the molecule. On the other hand, in contrast to HOMO, the LUMO of 2, 3,

Figure 2. Results of the highest occupied molecular orbital (HOMO) and the lowest occupied molecular orbital (LUMO) for compounds 1-6

mine the reactivity of compounds 1-6 when they interact with the researched protein, providing a profound insight into the chemical activities from a quantum mechanics perspective.³⁹ Figure 2 illustrates the Highest Occupied Molecular Orbital (HOMO) and Lowest Unoccupied Molecular Orbital (LUMO) of the optimized structures 1-6, and Table 1 shows the energy parameters of HOMO, LU-MO, and the energy gap between them. In drug develop-

5, and 6 is mainly distributed over the *trans*-feruloyl group,

and the LUMO of 1 and 4 also distributes over this group.

LUMO-3

LUMO-4

Table 1. HOMO and LUMO energies, binding affinity, and molecular interactions of isolated compounds from B. prionitis.

Compound	E _{HOMO}	E _{LUMO}	ΔΕ	ΔG_{dock}	Hydrogen bond interactions with residues	Hydrophobic interactions with residues
1	-6.052	-1.796	4.256	-9.084	Val604, Leu365, Arg415, Tyr334, Asn382, Asn387, Tyr572	TYR334, TYR525, ALA556
2	-5.982	-2.083	3.899	-9.097	SER363, TYR572, ARG415, LEU365	TYR525, TYR572, TYR334, ALA556, ARG415
3	-5.559	-2.021	3.537	-9.329	TYR334, ARG415, ILE416	TYR525, TYR572
4	-7.406	-0.995	6.411	-9.637	ASN387, GLN530	TYR334, ALA556, TYR572, PHE577
5	-7.084	-1.023	6.061	-9.639	ASN382, ILE416, VAL463, SER508	ARG415, ALA556, TYR525
6	-5.770	-2.032	3.738	-9.166	LEU365, ARG415, ARG483	ALA556, TYR525, GLY462

The phenylethanoid compounds (1-6) exhibit energy gaps of 4.256 eV, 3.899 eV, 3.537 eV, 6.412 eV, 6.061 eV, and 3.738 eV, respectively. A higher HOMO-LUMO energy gap indicates higher electron stability. As observed in Table 1, the highest energy gap is calculated for 4, while

the lowest HOMO-LUMO gap is seen in 3. Furthermore, the E_{HOMO} value of 3 is the highest, indicating its good electron-donating ability compared to the other compounds whereas the E_{LUMO} energy of 2 is the lowest, suggesting a good electron-accepting capability. Additionally,

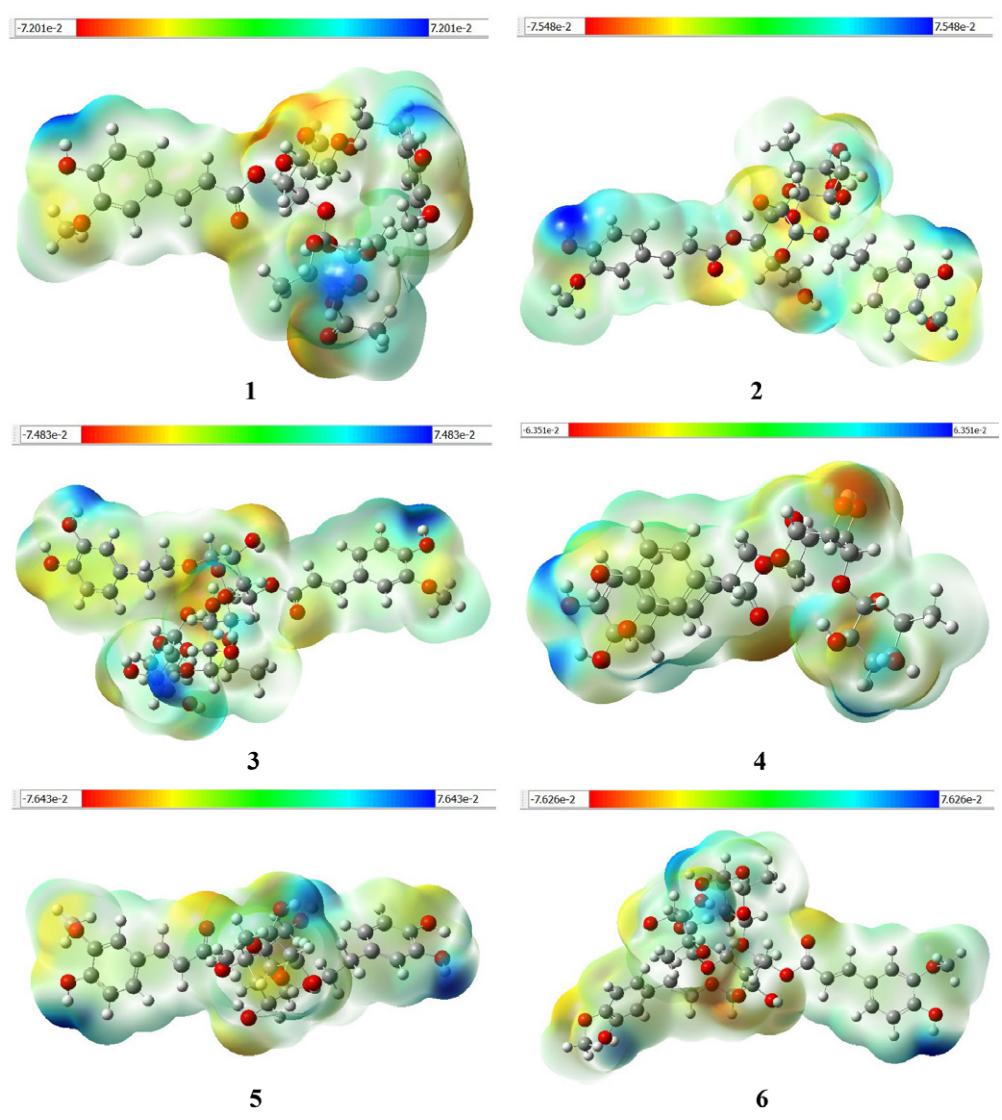


Figure 3. Results of the molecular electrostatic potential (MEP) for compounds 1-6

the phenylethanoids have $\rm E_{HOMO}$ values arranged in ascending order as 4 < 5 < 1 < 2 < 6 < 3, while the $\rm E_{LUMO}$ values indicate 2 < 6 < 3 < 1 < 5 < 4.

The Molecular Electrostatic Potential (MEP) map is established for the analysis and prediction of molecular behavior, used to identify electron-rich and electron-deficient sites as well as the potential to form hydrophobic interactions with target biological molecules.⁴⁰ This map indicates positive and negative regions on the molecule,

aiding in predicting interactions between the molecule and other molecules. Additionally, this method is extremely useful in determining the relationship between physical properties and molecular structure. The color scales in the MEP map represent the distribution of charge on the molecular surface, with red representing electron-rich regions (or electrophilic reactivity), while blue indicates electron-deficient regions (or nucleophilic reactivity). The gradual transition from navy blue to green, yellow, orange,

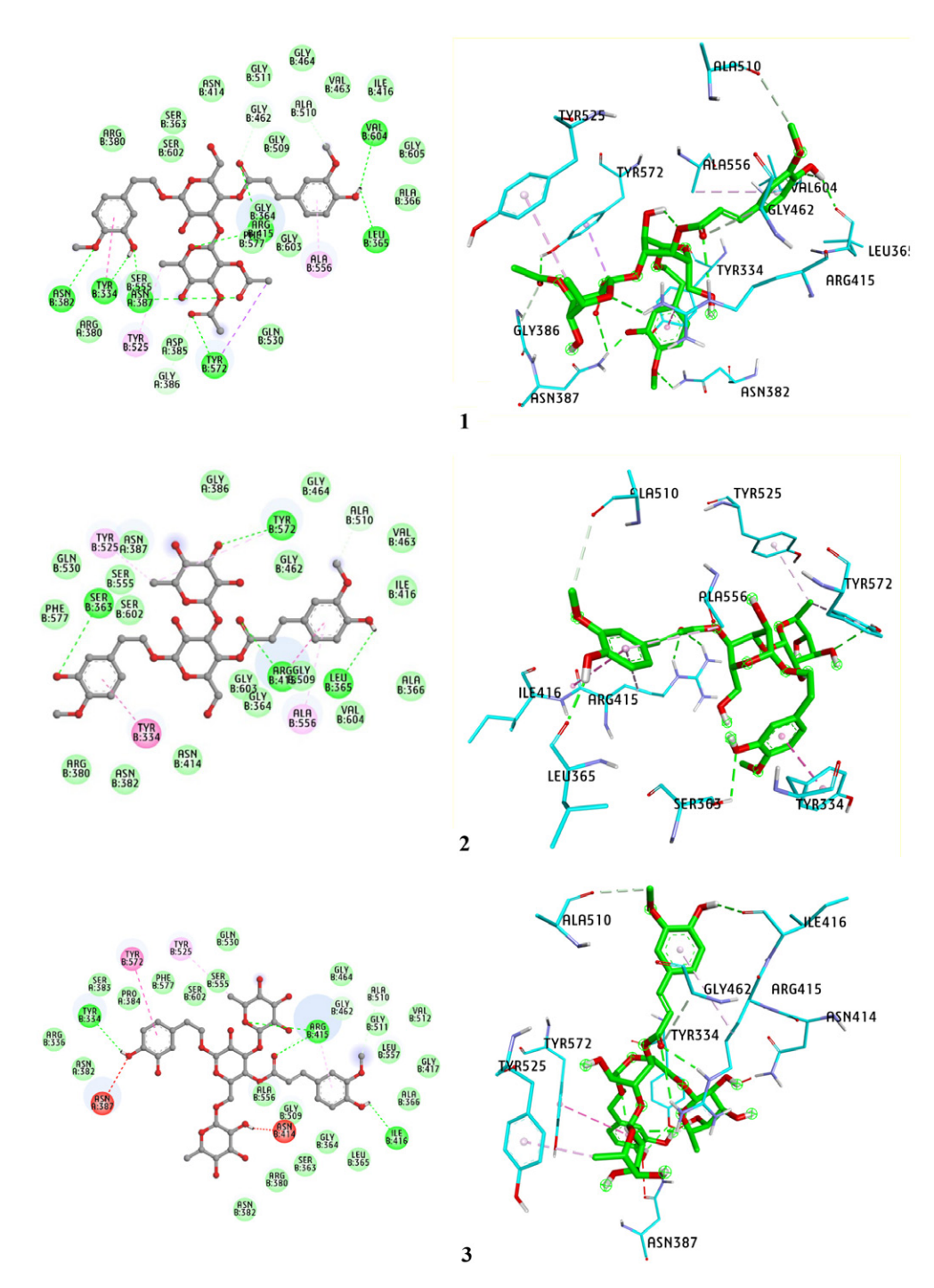
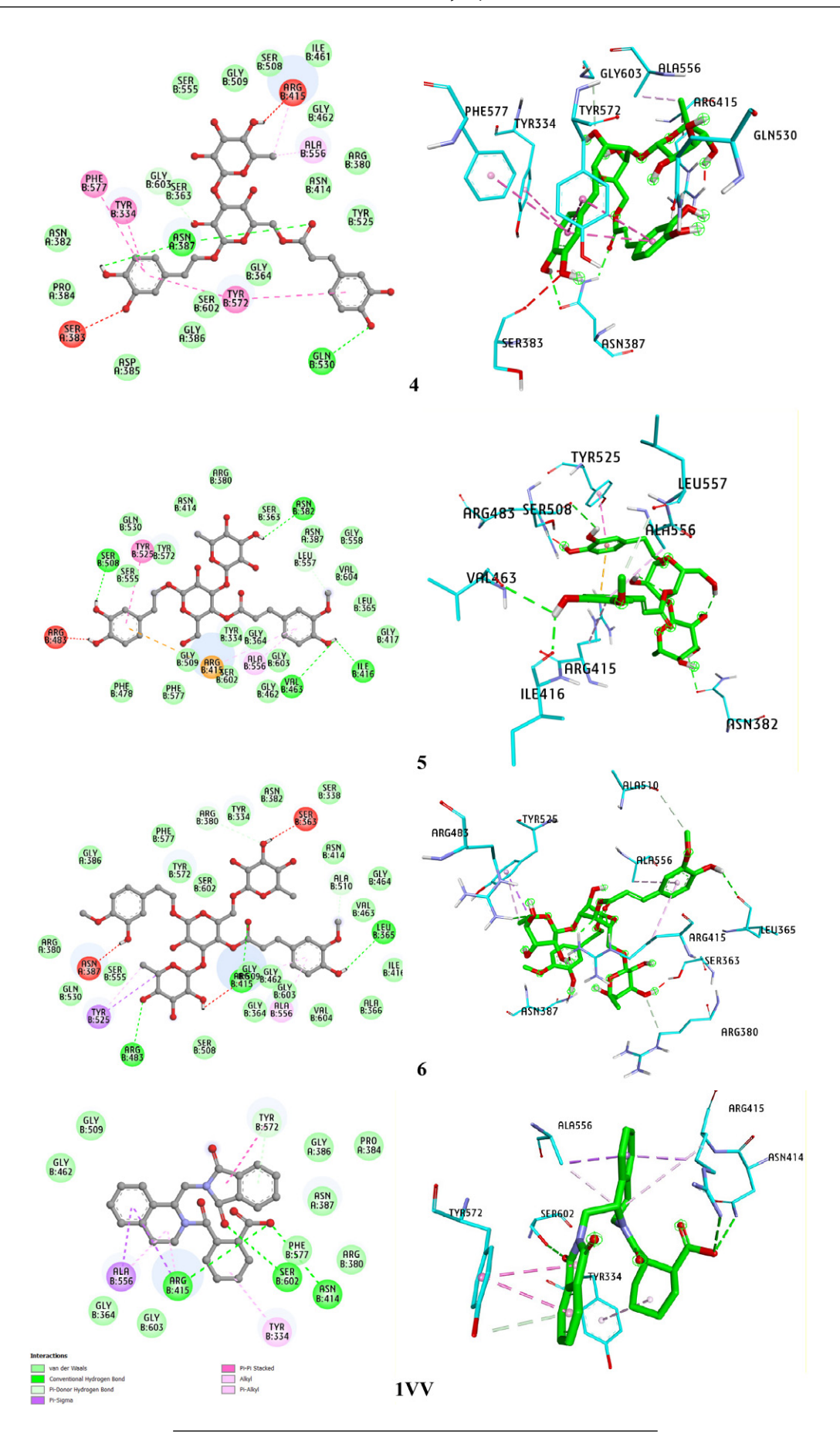


Figure 4. Molecular interactions of isolated compounds 1-6 with amino acid residues in the Keap1 active site.



 $\label{lem:community} \textbf{Keomanykham et al.:} \ \ \textit{Structures and Properties of Phenylethanoid Glycosides} \ \ \dots$

and red describes the electrostatic potential on the molecule's surface.

Based on the fully optimized geometry structure at the B3LYP/6-311G (d,p) theoretical level, MEP maps for all six isolated compounds were calculated. As detailed in Figure 3 analysis, high electronegative static regions concentrate on the oxygen atoms on the ring and ketone groups in phenylethanoids. Meanwhile, high electropositive regions primarily focus on the hydroxyl proton attached to C-3, feruloyl and caffeoyl substituents. The hydroxyl groups of phenylethanoids (1-6) act as electron-acceptor sites capable of forming hydrogen bonds with amino acid residues at protein binding sites and donating hydrogen atoms to free radicals. At these positions, the potential values for phenylethanoids (1-6) are 7.201×10^{-2} eV, 7.548 $\times 10^{-2} \text{ eV}$, $7.483 \times 10^{-2} \text{ eV}$, $6.351 \times 10^{-2} \text{ eV}$, $7.643 \times 10^{-2} \text{ eV}$, and 7.626×10^{-2} eV, respectively, indicating potential nucleophilic attack sites. Based on these findings, we can predict positions where nucleophilic and electrophilic attacks might occur, elucidating the assembly outcomes related to the hydrogen bonding and other interactions of each molecule with the amino acid residues at the active site of the studied protein.

3. 3. Docking and Oral Toxicity Prediction Results

The optimal geometry of isolated compounds (1-6) was further subjected to virtual screening on the potential antioxidant target Keap1. Prior to the screening process, the validation of the docking procedure was conducted, and the root-mean-square deviation (RMSD) value was determined to be 0.77 Å (< 2 Å), indicating a high reliability of the docking process (Figure S1).41 The binding mode of the crystallographically co-crystallized ligand (1S,2R)-2- $\{[(1S)-1-[(1,3-\text{dioxo}-1,3-\text{dihydro}-2H-\text{isoindol}-2-\text{yl})\}$ methyl]-3,4-dihydroisoquinolin-2(1H)-yl]carbonyl} cyclohexanecarboxylic acid (1VV) with the Keap1 active site was elucidated in Figure S1, and the results were consistent with previously reported data.²⁹ The binding affinity and protein-ligand interactions of the six phenylethanoids are detailed in Figure 4 and Table 1. The binding affinities of the investigated compounds demonstrated strong interactions with amino acid residues in the Keap1 active site, with ΔG_{dock} values ranging from -9.639 to -9.084 kcal/mol. Additionally, the interaction types and docked poses of compounds 1-6 were observed, as depicted in Figure 4 and S2. Specifically, compound 1 exhibited a binding affinity of -9.084 kcal/mol, forming seven hydrogen bonds with amino acid residues including Val604, Leu365, Arg415, Tyr334, Asn382, Asn387, and Tyr572. Moreover, hydrophobic interactions were observed for the Keap1-1 complex with Tyr525, Ala556 (π -alkyl interaction), Tyr334 (π - π stacked interaction), and Tyr572 (π - σ interaction). While compound 2 lacked acetyl groups at positions 2"-O- and 3"-O-, the ΔG_{dock} value showed minimal change ($\Delta G_{dock} = -9.097 \text{ kcal/mol}$).

Compound 2 also formed hydrogen bonds with Arg415, Leu365, and Tyr572 residues, and additionally, established hydrogen bonds with Ser363 and other hydrophobic interactions. The absence of a methyl group at position 4-O- in the molecule showed that compound 5 had the strongest binding affinity among the studied compounds with ΔG_{dock} = -9.639 kcal/mol. This was contributed by hydrogen bond interactions with amino acid residues Ser508, Asn382, Ile416, and Val463, as well as π - π stacked interactions with Tyr525, π -cation interactions with Arg415, and π -alkyl interactions with Tyr525 and Arg415 in the benzene ring. Compound 4, with an additional rhamnose moiety compared to compound 2, exhibited increased binding affinity $(\Delta G_{dock} = -9.637 \text{ kcal/mol})$, nearly equal to compound 5. In contrast to compound 4, the absence of a methyl group in compound 6 weakened its binding affinity. In terms of interactions in the Keap1 active site, compound 4 formed two hydrogen bonds with Asn387 and Gln530, while compound 6 established three hydrogen bonds with Arg415, Leu365, and Arg483. Finally, the docking result of compound 3 showed $\Delta G = -9.329$ kcal/mol. In the Keap1 active site, hydrogen bonds were formed between amino acid residues Tyr334, Arg415, and Ile416, and compound 3, in particular, it also exhibited π - π T-shape and π -alkyl interactions with Tyr572 and Tyr525, respectively. Notably, the complex of Keap1 with the co-crystallized compound 1VV revealed the formation of a hydrogen bond with the crucial residue Arg415, which was also observed in compounds 1, 2, 4, and **6**. Arg415 plays a crucial role in the active binding site of Keap1 with Nrf2, particularly in the P1 sub-pocket. Arg415, along with Arg483, is involved in electrostatic interactions with the substrate due to the highly positive charge of this pocket. These interactions are significant for the binding capability of Keap1, contributing to the maintenance of the interaction between Keap1 and Nrf2.⁴² This finding suggests that these compounds may have inhibitory potential similar to the co-crystallized compound 1VV. In addition, the potential toxicities of compounds 1-6 were predicted using the ProTox II website, as shown in Table S1. It can be observed that all tested compounds from the whole Barleria prionitis plant exhibited toxicity below the threshold of 5, with predicted LD₅₀ values of 5000 mg/kg, indicating low toxicity and high safety for oral consumption in humans. In the previous research, phenylethanoids also demonstrated effective inhibitory capabilities on Keap1.43 For instance, forsythoside B and alyssonoside were isolated from Callicarpa kwangtungensis, a traditional Chinese herb that could act as the inhibitors of Keap1-Nrf2 interaction via in vitro assay and molecular docking.44 Therefore, phenylethanoids isolated from B. prionitis may be potential candidates for future antioxidant biological tests.

3. 4. Biological Activities

B. prionitis has been widely used in the treatment of various diseases in traditional medicine and its crude ext-

racts also showed many good biological properties. In this section, we had evaluated the DPPH free radical scavenging activity of six pure compounds, isolated from *B. prionitis* (Table 1). All of these compounds **1-6** were found to be strong to moderate antioxidant active in this assay with an IC₅₀ value in the range of 110–389 μ M. Among them, isoaceteoside (**4**) showed the strongest activity with its IC₅₀ value of 110.91 \pm 2.48 μ M as compared to positive control, ascorbic acid (IC₅₀ 158.82 \pm 8.97 μ M). As mentioned in the previous section, the docking results suggest that the isolated compounds (**1-6**) have the ability to effectively inhibit the Keap1 protein, which is associated with antioxidant activity. This indicates that the two approaches (molecular docking and the DPPH assay) provide a more comprehensive understanding of the antioxidant efficacy of the studied compounds.

Table 2. DPPH free radical scavenging activity of compounds 1-6

Compound	IC ₅₀ value (μM)	Compound	IC ₅₀ value (μM)
1	389.43 ± 55.85	5	296.57 ± 12.02
2	327.07 ± 11.81	6	338.37 ± 34.57
3	239.68 ± 20.40	Ascorbic	158.82 ± 8.97
4	110.91 ± 2.48	acid	

4. Conclusions

Six secondary metabolites, acetylmartynoside A (1), martynoside (2), 3-O-methylpoliumoside (3), isoaceteoside (4), leucosceptoside A (5), and 2-(3-hydroxy-4-methoxyphenyl)-ethyl-O-(α -L-rhamnosyl)-(1 \rightarrow 3)-O-(α -L-rhamnosyl)-(1 \rightarrow 6)-4-O-(E)-feruloyl- β -D-glucopyranoside (6), isolated from the Laotian medicinal plant *Barleria prionitis* Linn, were evaluated for their antioxidant activity. Their effectiveness was assessed both *in vitro* through DPPH radical scavenging assays and *in silico* via molecular docking against the Keap1 protein. Thus, it is possible to apply this methodology to discovering antioxidant constituents in natural products.

Data Availability

All spectral data, figures S1, S2 and table S1 are uploaded as Supplementary Materials

Acknowledgements

This research is funded by Vietnam National Foundation for Science and Technology Development (NAFOSTED) under grant number 104.01-2021.44.

Conflict of Interest

The authors declare no conflict of interest, financial or otherwise.

5. References

- R. N. Chopra, S. L. Nayar, I. C. Chopra: In Glossary of Indian Medicinal Plants, CSIR. New Delhi, 1965.
- H. M. Gupta, V. K. Saxena, Nat. Acad. Sci. Lett. 1984, 7, 187– 189.
- N. Mark, K. Sounthone, S. Bouakhaykhone, T. Philip, S. Khamphone, L. Vichith, A. Kate: A checklist of the vascular plants of Lao PDR, Royal Botanic Garden Edinburgh, Edinburgh, 2007.
- K. L. Tran: Acanthaceae. Checklist of plant species of Vietnam, Publishing House of Agriculture, Hanoi, 2005.
- 5. T. L. Do: Vietnamese Traditional Medicinal Plants and Drugs, 3rd Ed. Publishing House of Medicine, Hanoi, **2001**.
- S. Onvilay, S. Muachanh, P. Khamman: Medicinal Plants of the Ex-situ Medicinal Plants Preserve in Veunkham, Institute of Traditional Medicine (ITM), Ministry of Health, Vientiane, 2019.
- P. Khare: Indian Medicinal Plants: An Illustrated Dictionary, 1st Ed. Springer Science, New York, 2007.

DOI:10.1007/978-0-387-70638-2_227

- A. Ata, K. S. Kalhari, R. Samarasekara, *Phytochem. Lett.* 2009, 2, 37–40. DOI:10.1016/j.phytol.2008.11.005
- J. L. Chen, P. Blanc, C. A. Stoddart, M. Bogan, E. J. Rozhon, N. Parkinson, Z. Ye, R. Cooper, M. Balick, W. Nanakorn, M. R. Kernan, J. Nat. Prod. 1998, 61, 1295–1297.
 DOI:10.1021/np980086y
- 10. M. Daniel: Medicinal Plants: Chemistry and Properties, 1st Ed. Science Publishers, USA, **2006**.
- K. S. Kosmulalage, S. Zahid, C. C Udenigwe, S. Akhtar, A. Ata, *Naturforsc. B.* 2007, 62, 580–586.
 DOI:10.1515/znb-2007-0417
- S. O. Amoo, A. R. Ndhlala, J. F. Finnie, J. Van Staden, S. Afr. J. Bot. 2011, 77, 435–445. DOI:10.1016/j.sajb.2010.11.002
- 13. K. R. Aneja, R. Joshi, C. Sharma, N. Y. Acad. Sci. **2010**, 3, 5–12.
- B. V. Ghule, P. G. Yeole, J. Ethnopharmacol. 2012, 141, 424–431. DOI:10.1016/j.jep.2012.03.005
- P. Panchal, S. Meena, K. Singh, N. Sharma, *Int. J. Pharm. Pharm. Sci.* 2018, 10, 100–103.

DOI:10.22159/ijpps.2018v10i10.27967

B. Singh, S. Bani, D. K. Gupta, B. K. Chandan, A. Kaul, *J. Eth-nopharmacol.* 2003, 85, 187–193.

DOI:10.1016/S0378-8741(02)00358-6

- B. Singh, B. K. Chandan, A. Prabhakar, S. C. Taneja, J. Singh,
 G. N. Qazi, *Phytother. Res.* 2005, 19, 391–404.
 DOI:10.1002/ptr.1509
- 18. A. Yadav, S. Mohite, Int. J. Sci. Res. Chem. 2020, 5, 50-58.
- S. Bharadwaj, S. A. El-Kafrawy, T. A. Alandijany, L. H. Bajrai,
 A. A. Shah, A. Dubey, A. K. Sahoo, U. Yadava, M. A. Kamal,
 E. I. Azhar, S. G. Kang, V. D. Dwivedi, *Viruses* 2021, *13*, 305.
 DOI:10.3390/v13020305
- T. C. Yadav, N. Kumar, U. Raj, N. Goel, P. K. Vardawaj, R. Prasad, V. Pruthi, *J. Biomol. Struct. Dyn.* 2020, 38, 382–397.
 DOI:10.1080/07391102.2019.1575283
- 21. L. Yang, H. Zeng, X. Xia, H. Wang, B. Zhao, J. He, Bioorg.

- *Chem.* **2022**, *129*, 106165. **DOI:**10.1016/j.bioorg.2022.106165
- M. A. Loza-Mejía, J. R. Salazar, J. F Sánchez-Tejeda, *Biomolecules* 2018, 8, 121. DOI:10.3390/biom8040121
- M. Bernardi, M. R. Ghaani, O. Bayazeid, J. Mol. Model. 2021, 27, 1–8. DOI:10.1007/s00894-021-04963-2
- 24. C. S. Bertanha, V. M. M. Gimenez, R. A. Furtado, D. C. Tavares, W. R. Cunha, M. L. A. Silva, A. H. Januario, A. Borges, D. F. Kawano, R. L. T. Parreira, P. M. Pauletti, *J. Braz. Chem. Soc.* 2020, 31, 849–855.
- G. Culletta, B. Buttari, M. Arese, S. Brogi, A. M. Almerico, L. Saso, M. Tutone, *Eur. J. Med. Chem.* 2024, 116355.
 DOI:10.1016/j.ejmech.2024.116355
- D. T. T. Giang, T. T. Hieu, N. H. Tuan, N. X. Ha, N. D. Khoa, N. M. Chanh, N. T. T. Hien, V. T. Thuan, T. T. T. Hang, N. T. T. Giang, H. V. Trung, J. Essent. Oil-Bear. Plant 2024, 27, 1439–1448. DOI:10.1080/0972060X.2024.2418850
- 27. C. Yu, J. H. Xiao, Oxid. Med. Cell Longev. 2021, 6635460.
- M. J. Frisch et al., Gaussian 09, Revision A.02, Gaussian, Inc. Wallingford CT, 2016.
- 29. E. Jnoff, C. Albrecht, J. J. Barker, O. Barker, E. Beaumont, S. Bromidge, F. Brookfield, M. Brooks, C. Bubert, T. Ceska, V. Corden, G. Dawson, S. Duclos, T. Fryatt, C. Genicot, E. Jigorel, J. Kwong, R. Maghames, I. Mushi, R. Pike, Z. A. Sands, M. A. Smith, C. C. Stimson, J. P. Courade, *ChemMedChem* 2014, 9, 699–705. DOI:10.1002/cmdc.201300525
- J. Eberhardt, D. Santos-Martins, A. F. Tillack, S. Forli, J. Chem. Inf. Model. 2021, 61, 3891–3898.
 DOI:10.1021/acs.jcim.1c00203
- P. Banerjee, E. Kemmler, M. Dunkel, R. Preissner, *Nucleic Acids Res.* 2024, 46, W257–W263.
 DOI:10.1093/nar/gky318

- 32. M. S. Blois, *Nature* **1958**, *181*, 1199–1200. **DOI:**10.1038/1811199a0
- S. G. Leitão, M. A. Kaplan, F. D. Monache, J. Nat. Prod. 1994, 57, 1703–1707. DOI:10.1021/np50114a013
- E. Tayfun, T. Deniz, C. Ihsan, M. I. Chris, *Turk. J. Chem.* 2002, 26, 465–471.
- M. Mostafa, N. Nahar, M. Mosihuzzaman, T. Makhmoor,
 M. I. Choudhary, A. U. Rahman, *Nat. Prod. Res.* 2007, 21, 354–361. DOI:10.1080/14786410701194401
- R. W. Owen, R. Haubner, W. Mier, A. Giacosa, W. E. Hull,
 B. Spiegelhalder, H. Bartsch, Food Chem. Toxicol. 2003, 41,
 703–717. DOI:10.1016/S0278-6915(03)00011-5
- T. Miyase, A. Koizumi, A. Ueno, T. Noro, M. Kuroyanagi, S. Fukushima, Y. Akiyama, T. Takemoto, *Chem. Pharm. Bull.* 1982, 30, 2732–2737. DOI:10.1248/cpb.30.2732
- B. N. Zhou, B. D. Bahler, G. A. Hofmann, M. R. Mattern, R. K. Johnson, D. G. I. J. Kingston, *J. Nat. Prod.* 1998, 61, 1410–1412. DOI:10.1021/np980147s
- M. Özcan, I. Dehri, M. Erbil, *Appl. Surf. Sci.* 2004, 236, 155–164. DOI:10.1016/j.apsusc.2004.04.017
- 40. N. Ye, Z. Yang, Y. Liu, *Drug Discov. Today* **2022**, *27*, 1411–1419. **DOI**:10.1016/j.drudis.2021.12.017
- V. T. T. Le, H. V. Hung, N. X. Ha, C. H. Le, P. T. H. Minh, D. T. Lam, *Molecules* 2023, 28, 7253.
 DOI:10.3390/molecules28217253
- 42. M. C. Lu, J. A. Ji, Z. Y. Zhang, Q. D. You, Med. Res. Rev. 2016, 36, 924–963. DOI:10.1002/med.21396
- J. Hong, Z. Shi, C. Li, X. Ji, S. Li, Y. Chen, G. Jiang, M. Shi, W. Wang, Y. Zhang, B. Hu, S. Yan, *Free Radical Biol. Med.* 2021, 171, 365–378. DOI:10.1016/j.freeradbiomed.2021.05.020
- A. Wu, Z. Yang, Y. Huang, H. Yuan, C. Lin, T. Wang, Z. Zhao,
 Y. Zhao, C. Zhu, J. Ethnopharmacol. 2020, 258, 112857.
 DOI:10.1016/j.jep.2020.112857

Povzetek

Iz cele rastline *Barleria prionitis* Linn smo prvič izolirali šest feniletanoidnih glikozidov: acetilmartinozid A (1), martinozid (2), 3-O-metilpoliumozid (3), izoaceteozid (4), levkoskeptozid A (5) in 2-(3-hidroksi-4-metoksifenil)-etil-O-(α-L-ramnozil)-(1 \rightarrow 3)-O-(α-L-ramnozil)-(1 \rightarrow 6)-4-O-E-feruloil- β -D-glukopiranozid (6). Njihove strukture smo določili s pomočjo 1D in 2D NMR ter masne spektrometrije. Poleg tega smo raziskali antioksidativno aktivnost navedenih spojin. Vse spojine so pokazale zaviralne učinke na protein Keap1, pri čemer so imele ocenjene vezavne afinitete v območju od –9,639 do –9,084 kcal/mol z metodo molekularnega sidranja. Prav tako so imele zmerno sposobnost lovljenja prostih radikalov DPPH, pri čemer so njihove IC50 vrednosti znašale med 110 in 389 μM. Za vse spojine smo ocenili toksičnost na stopnjo 5 z visokimi vrednostmi LD50 (LD50 = 5000 mg/kg), kar kaže na nizko toksičnost in visoko varnost za peroralno uživanje pri ljudeh.



Except when otherwise noted, articles in this journal are published under the terms and conditions of the Creative Commons Attribution 4.0 International License